Electronic Supplementary Material (ESI) for Environmental Science: Nano.

Supporting Information

Controllable synthesis of the defect-enriched MoO_{3-x} nanosheets as an effective visible-light photocatalyst for the degradation of organic dyes

Yuqi Zhang[a#], Xiang Yu[a,b#], Huan Liu[a], Xinyi Lian[a], Bin Shang[a], Yue Zhan[a], Tingting Fan[a], Zhou Chen[a]* and Xiaodong Yi[a]*

a. College of Chemistry and Chemical Engineering, College of Materials, Xiamen University, Xiamen 361005, P. R. China.

b. Inorganic Chemistry and Catalysis Group, Debye Institute for Nanomaterials Science, Utrecht University, Utrecht, The Netherlands.

***Corresponding authors**:

xdyi@xmu.edu.cn (X. D. Yi), zhouchen@xmu.edu.cn (Z. Chen).

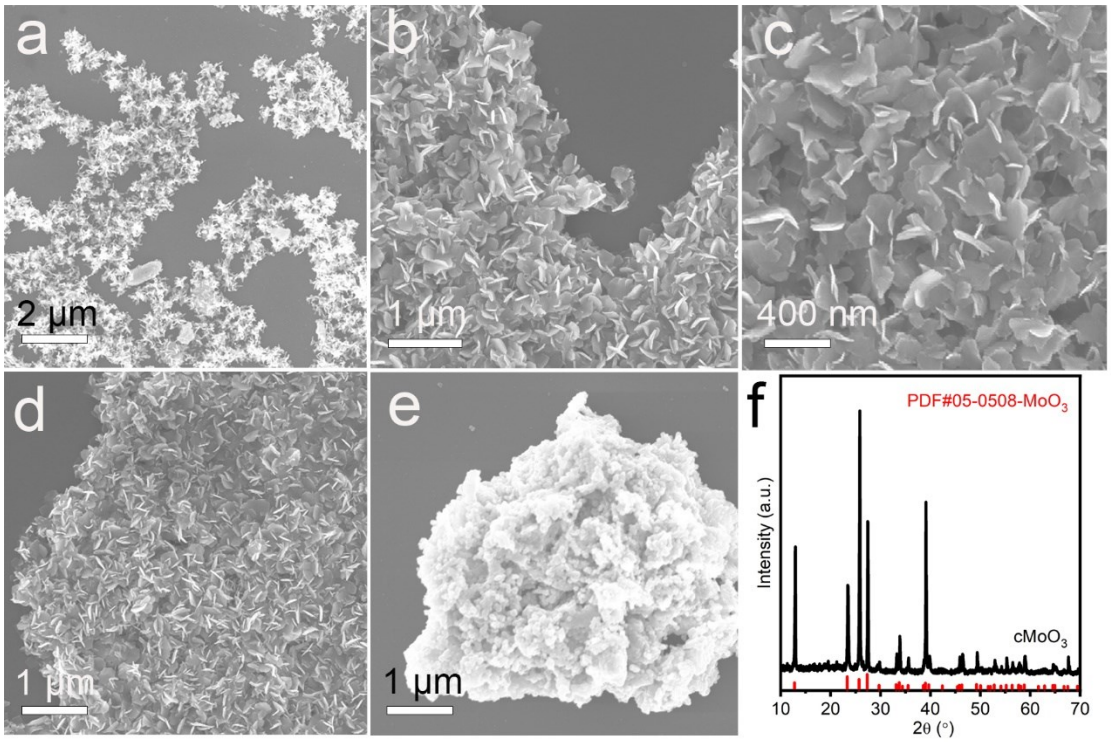

Fig. S1. Morphology analysis of MoO_{3-x} nanosheets. The SEM images of (a) MoO_{3-x}-2, (b) MoO_{3-x}-4, (c) MoO_{3-x}-8, (d) MoO_{3-x}-12 and (e) $cMoO_3$; (e) XRD pattern of $cMoO_3$.

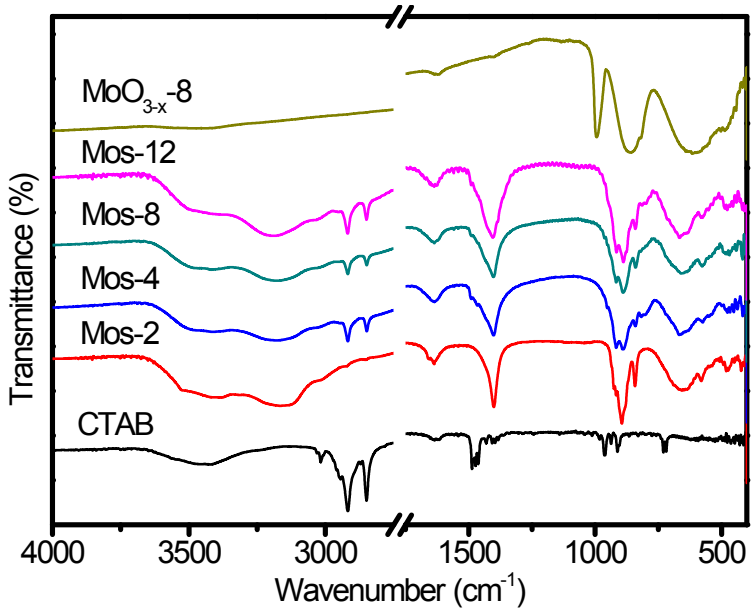

Fig. S2. FTIR spectra of ammonium molybdate nanosheets (Mos), CTAB and MoO_{3-x}-8. The Mos-a are the samples collected before thermal treatment ("a" equals 2, 4, 8 and 12).

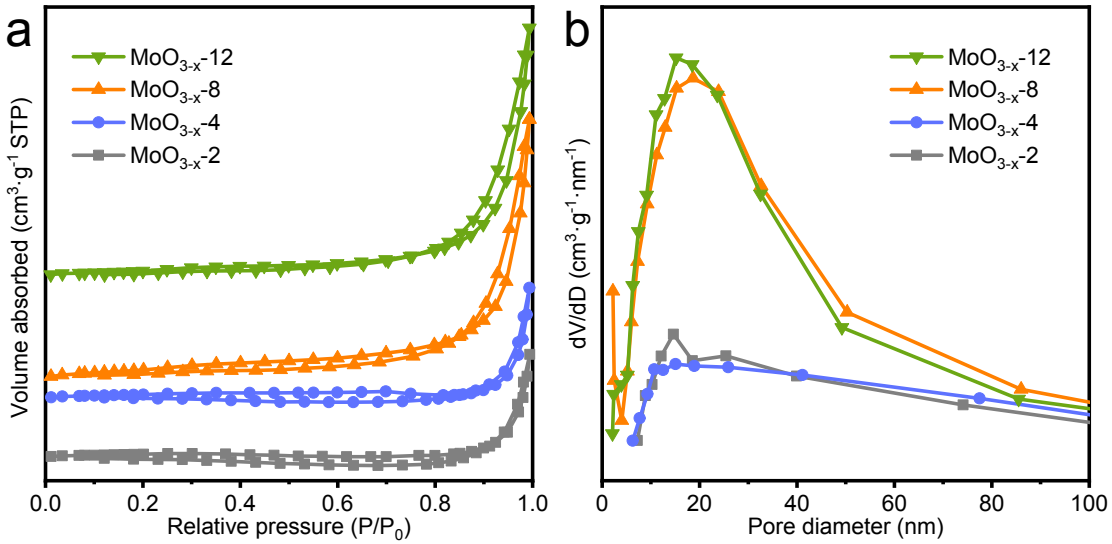

Fig. S3. (a) Nitrogen adsorption-desorption isotherms (b) BJH pore size distribution curves of MoO_{3-x} nanosheets.

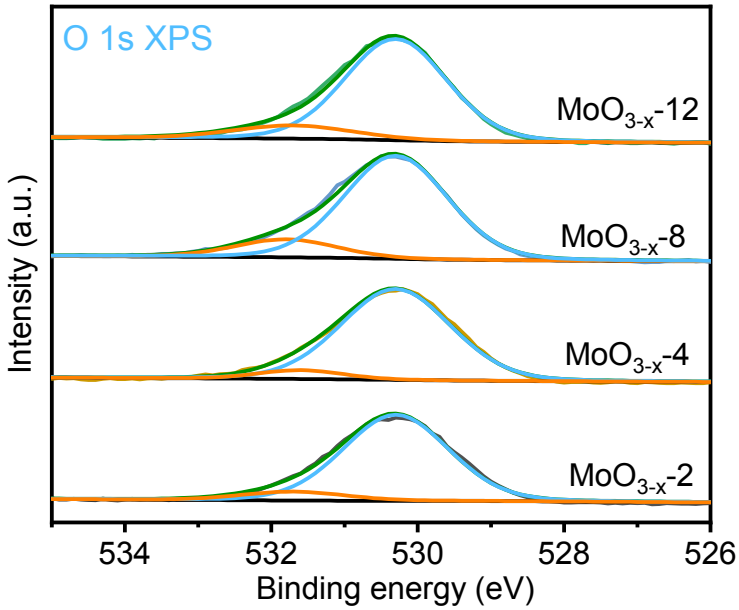

Fig. S4. The high resolution O 1s XPS spectra of MoO_{3-x}-2, MoO_{3-x}-4, MoO_{3-x}-8 and MoO_{3-x}-12.

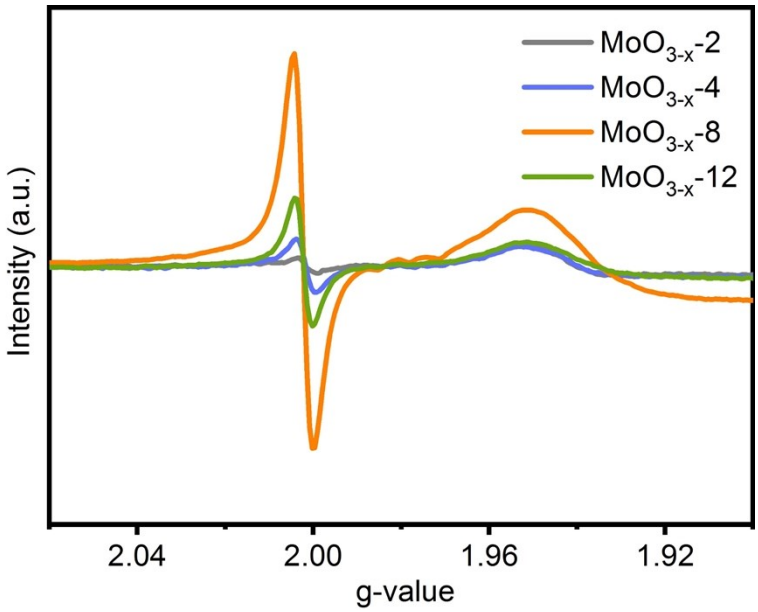

Fig. S5. ESR spectra of MoO_{3-x}-2, MoO_{3-x}-4, MoO_{3-x}-8 and MoO_{3-x}-12 (different batches of samples).

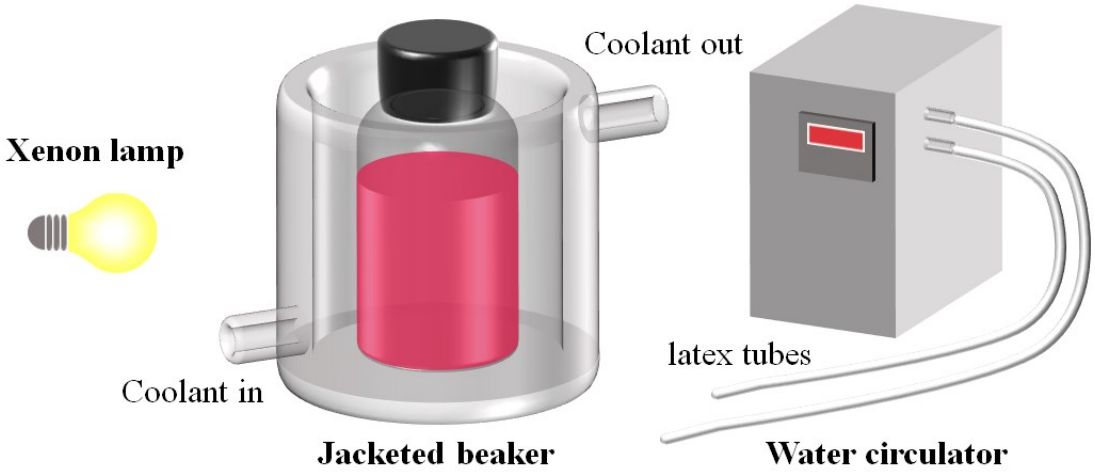

Fig. S6. The schematic diagram of the photocatalytic device.

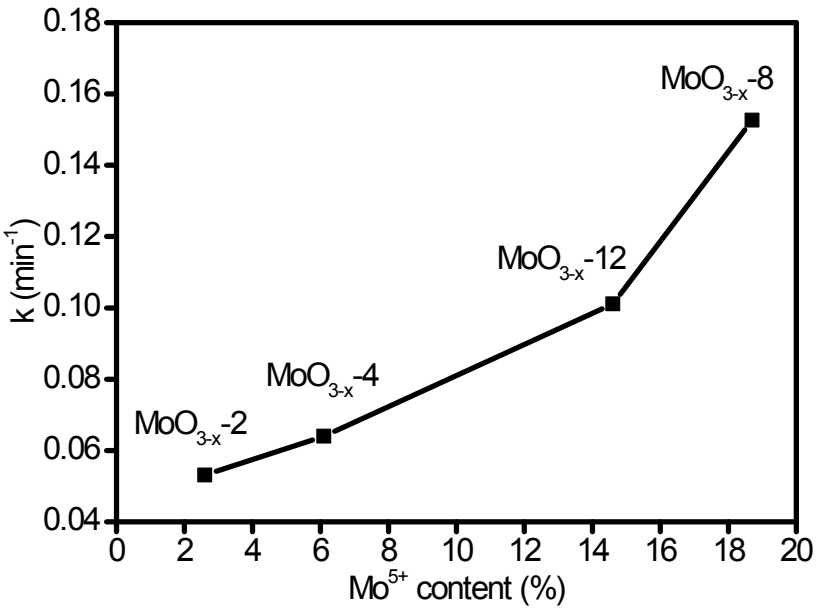

Fig. S7. The plots between Mo^{5+} concentration and the rate constant of MoO_{3-x} photocatalysts.

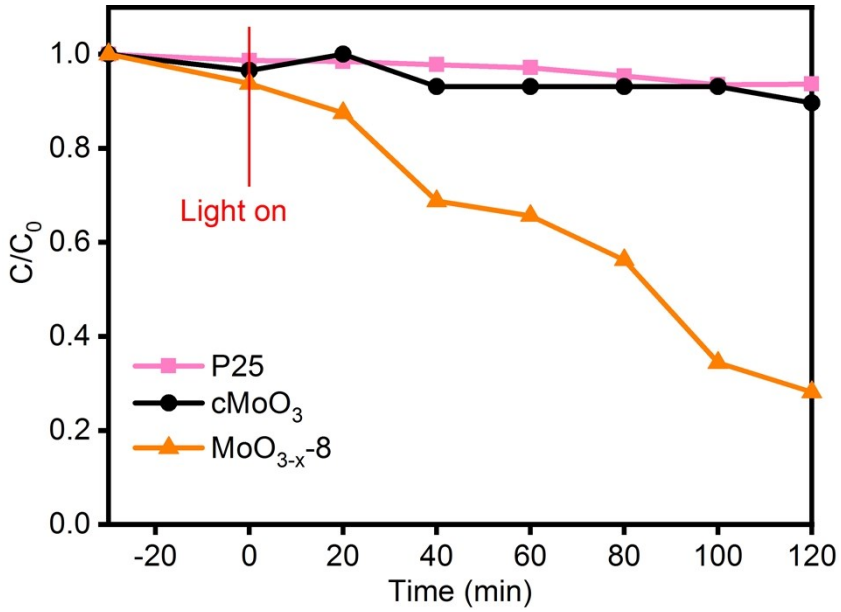

Fig. S8. The degradation of phenol over P25, $cMoO_3$ and MoO_{3-x}-8 under visible light.

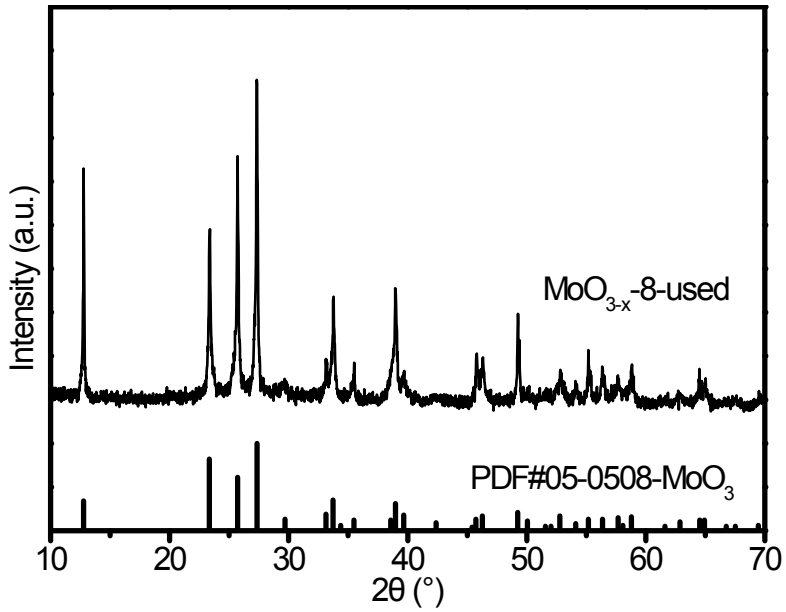

Fig. S9. The XRD pattern of the MoO_{3-x}-8-used catalyst.

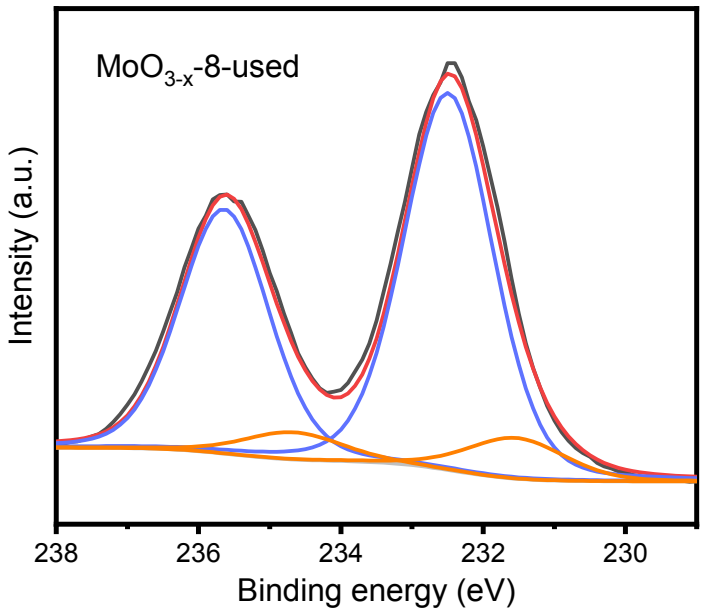

Fig. S10. The XPS of the MoO_{3-x}-8-used catalyst.

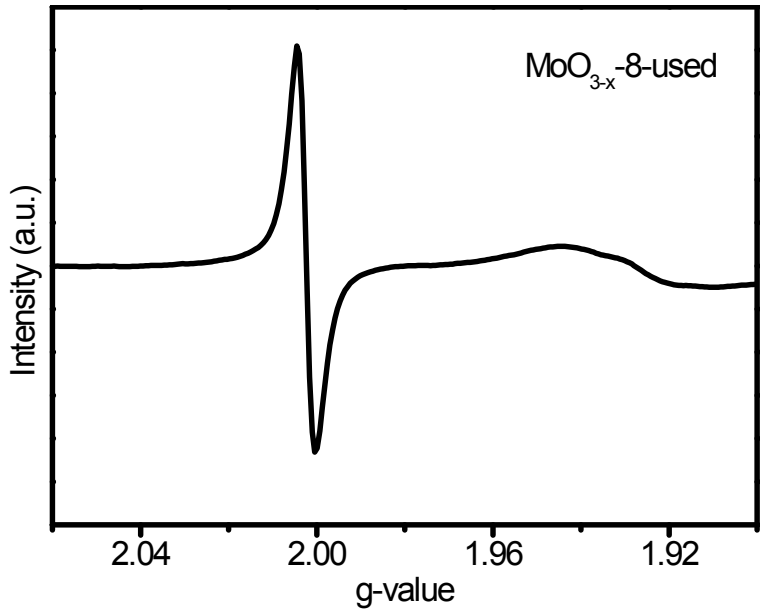

Fig. S11. The ESR of the MoO_{3-x}-8-used catalyst.

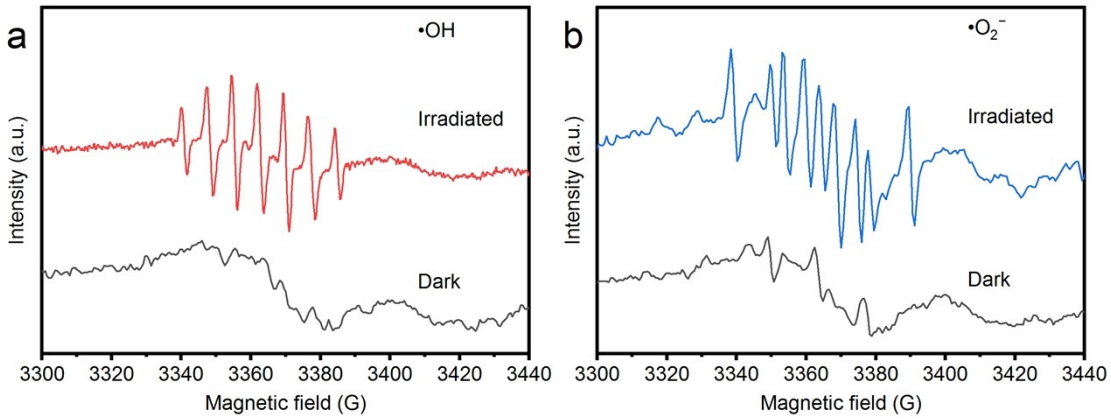

Fig. S12. ESR spectra of (a) DMPO-•OH and (b) DMPO-•O_2^- adducts for MoO_{3-x}-8 under visible-light irradiation.

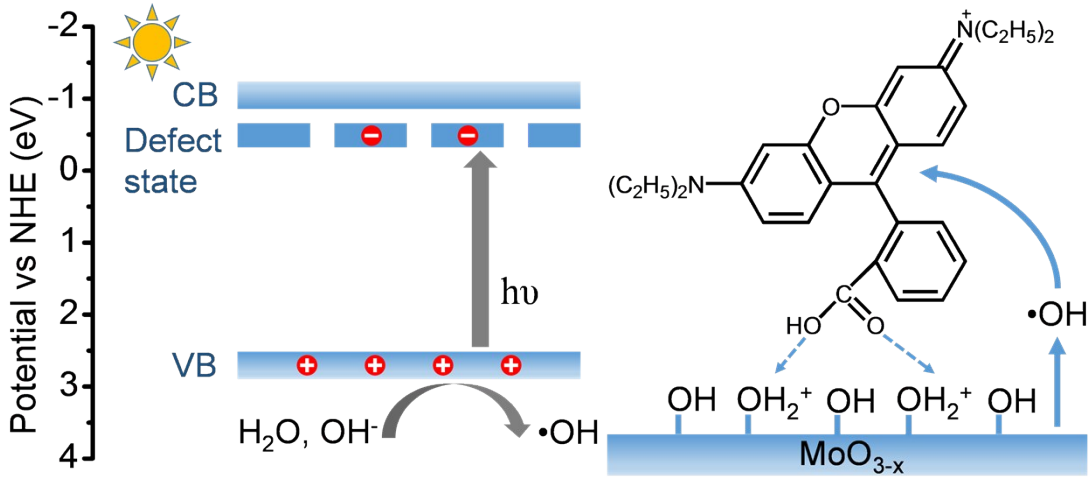

Fig. S13. The proposed band structure and the photodegradation mechanism of MoO_{3-x} nanosheets.

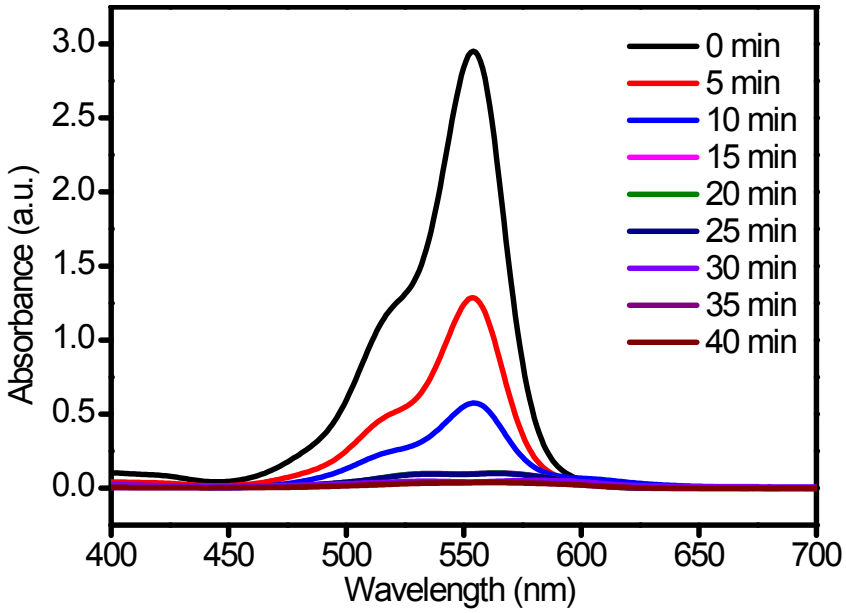

Fig. S14. UV–vis absorption spectra of RhB aqueous solution in the presence of MoO_{3-x}-8 under visible-light irradiation.

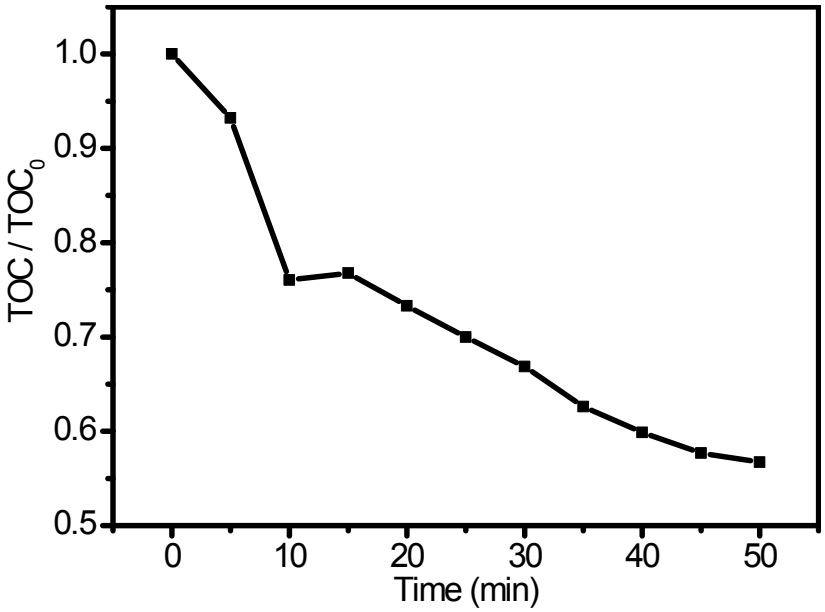

Fig. S15. TOC removal of the RhB solution by the MoO_{3-x}-8 photocatalyst.

Table S1. BET specific surface areas, average pore volumes and pore sizes of MoO_{3-x} samples.

Samples	BET surface area (m^2/g)	Pore volume (cm^3/g)	Pore size (nm)
MoO_{3-x}-2	6.3	0.024	37.2
MoO_{3-x}-4	5.7	0.025	39.5
MoO_{3-x}-8	11.7	0.058	25.1
MoO_{3-x}-12	10.1	0.056	24.4

Table S2. The C, N and H composition of MoO_{3-x}-2, MoO_{3-x}-4, MoO_{3-x}-8 and MoO_{3-x}-12 determined by organic elemental analysis.

Samples	Content of element (wt. %)		
	C	N	H
MoO_{3-x}-2	0.0	0.0	1.0
MoO_{3-x}-4	0.0	0.0	0.5
MoO_{3-x}-8	0.0	0.0	0.7
MoO_{3-x}-12	0.1	0.0	0.8

Table S3. The deconvolution results of Mo 3d XPS spectra of MoO_{3-x}-2, MoO_{3-x}-4, MoO_{3-x}-8 and MoO_{3-x}-12.

Samples	Atomic percentage (%)		Mo:O
	Mo^{5+}	Mo^{6+}	
MoO_{3-x}-2	2.6	97.4	1:2.99
MoO_{3-x}-4	6.1	93.9	1:2.98
MoO_{3-x}-8	18.7	81.3	1:2.93
MoO_{3-x}-12	14.6	85.4	1:2.94

Table S4. The photocatalytic rates of MoO_{3-x} samples expressed as reaction rate constant per unit BET surface area.

Photocatalysts	BET surface area (m^2/g)	k (min^{-1})	k' ($min^{-1} \cdot m^{-2}$)
MoO_{3-x}-2	6.3	0.0531	0.0084
MoO_{3-x}-4	5.7	0.0640	0.0112
MoO_{3-x}-8	11.7	0.1526	0.0130
MoO_{3-x}-12	10.1	0.1011	0.0100

Table S5. Recently published MoO_3 materials towards photocatalytic degradation RhB.

Catalysts	C(cat.) (g/L)	C(RhB) (mg/L)	Light source	Time (min)	Degradation rate (%)	Reference
MoO_{3-x}	1.6	47.6	150W LED lamp	10	40	[1]
$AgBr/MoO_3$	0.2	10	250 W Xenon lamp	5	95	[2]
MoO_{3-x}	0.6	20	300W xenon lamp（λ > 420 nm)	90	81	[3]
MoO_2/MoO_3	0.1	10	250 W Xenon lamp（λ > 400 nm)	30	90	[4]
dr-MoO_3	0.3	21	350W xenon lamp（λ > 400 nm)	50	95	[5]
MoO_3	0.6	30	150 W halogen lamp	60	99	[6]
MoO_3-CdS	2	10	300W xenon lamp（λ > 400 nm)	180	97	[7]
g-C_3N_4/α-MoO_3	0.3	10	250W xenon lamp（λ > 400 nm)	120	72	[8]
$BaTiO_3/MoO_3$	-	-	150 W halogen lamp	30	86	[9]
MoO_{3-x}-8	0.6	40	300W xenon lamp（λ > 420 nm)	15	95	This work

Reference

[1] A.S. Etman, H.N. Abdelhamid, Y.Y. Yuan, L.G. Wang, X.D. Zou and J.L. Sun, Facile water-based strategy for synthesizing MoO_{3-x} nanosheets: efficient visible light photocatalysts for dye degradation, ACS Omega, 2018, **3**, 2193-2201.

[2] B. Feng, Z.Y. Wu, J.S. Liu, K.J. Zhu, Z.Q. Li, X. Jin, Y.D. Hou, Q.Y. Xi, M.Q. Cong, P.C. Liu and Q.L. Gu, Combination of ultrafast dye-sensitized-assisted electron transfer process and novel Z-scheme system: AgBr nanoparticles interspersed MoO_3 nanobelts for enhancing photocatalytic performance of RhB, Appl. Catal. B: Environ., 2017, **206**, 242-251.

[3] Q.W. Liu, Y.W. We, J.W. Zhang, K.J. Chen, C.J. Huang, H. Chen and X.Q. Qiu, Plasmonic MoO_{3-x} nanosheets with tunable oxygen vacancies as efficient visible light responsive photocatalyst, Appl. Surf. Sci., 2019, **490**, 395-402.

[4] Q.Y. Xi, J.S. Liu, Z.Y. Wu, H.F. Bi, Z.Q. Li, K.J. Zhu, J.J. Zhuang, J.X. Chen, S.L. Lu, Y.F. Huang and G.M. Qian, In-situ fabrication of MoO_3 nanobelts decorated with MoO_2 nanoparticles and their enhanced photocatalytic performance, Appl. Surf. Sci., 2019, **480**, 427-437.

[5] B.J. Zheng, Z.G. Wang, X.Q. Wang and Y.F. Chen, Enhanced photocatalytic properties of defect-rich α-MoO_3 nanoflakes by cavitation and pitting effect, J. Hazard. Mater., 2019, **378**, 1-8.

[6] Y. Liu, P.Z. Feng, Z. Wang, X.Y. Jiao and F. Novel fabrication and enhanced photocatalytic MB degradation of hierarchical porous monoliths of MoO_3

nanoplates, Akhtar, Sci Rep, 2017, **7**, 1845.

[7] Z.Y. Shen, G. Chen, Y.G. Yu, Q. Wang, C. Zhou, L.X. Hao, Y.X. Li, L.M. He and R.D. Mu, Sonochemistry synthesis of nanocrystals embedded in a MoO_3-CdS core-shell photocatalyst with enhanced hydrogen production and photodegradation, J. Mater. Chem., 2012, **22**, 19646-19651.

[8] X.N. Zhang, J.J. Yi, H.X. Chen, M. Mao, L. Liu, X.J. She, H.Y. Ji, X.Y. Wu, S.Q. Yuan, H. Xu and H.M. Li, J. Construction of a few-layer g-C_3N_4/α-MoO_3 nanoneedles all-solid-state Z-scheme photocatalytic system for photocatalytic degradation, Energy Chem., 2019, **29**, 65-71.

[9] K.V. Alex, A. Prabhakaran, A.R. Jayakrishnan, K. Kamakshi, J.P.B. Silva and K.C. Sekhar, Charge coupling enhanced photocatalytic activity of $BaTiO_3$/MoO_3 heterostructures, ACS Appl. Mater. Interfaces, 2019, **11**, 40114-40124.